Reduced-order modelling and parameter estimation for a quarter-car suspension system

C Kim and **P I Ro***
Department of Mechanical and Aerospace Engineering, North Carolina State University, Raleigh, North Carolina, USA

Abstract: This paper presents a new approach to obtaining an accurate simple model for complex mechanical systems. The methodology is applied to a quarter-car suspension system with complex linkage structures. Firstly, a multi-body dynamic model which includes kinematic characteristics is developed. Using a linearization technique, a 32-state linear model for a quarter-car system is obtained. Secondly, model reduction techniques are applied to find a reasonable reduced-order model. The result of the model reduction shows the validity of the two-mass model given that the parameters are correctly identified. The paper presents both an analytical and an experimental way of identifying the parameters of the two-mass system based on the reduced-order model. The identified parameters are shown to vary significantly from component data typically used for the two-mass system depending on kinematic structures of the suspension system. The modelling procedures outlined in this paper provide a precise and efficient way of designing active suspension systems that minimizes a necessary tuning process.

Keywords: reduced-order model, quarter-car suspension, identification, equivalent parameters

NOTATION

a_i, b_i	coefficients of transfer function
$\mathbf{A}, \mathbf{B}, \mathbf{C}, \mathbf{G}$	system matrices of original model
$\mathbf{A}_b, \mathbf{B}_b, \ldots$	system matrices of the balanced system
$\mathbf{A}_m, \mathbf{B}_m, \ldots$	system matrices after modal transformation
$\mathbf{A}_r, \mathbf{B}_r, \ldots$	system matrices of the reduced-order model
$\mathbf{A}_s, \mathbf{B}_s, \mathbf{G}_s$	system matrices of two-mass model
$\bar{\mathbf{A}}_s, \bar{\mathbf{B}}_s, \bar{\mathbf{G}}_s$	system matrices of modified reduced-order model
b_s	damping rate of strut (N s/m)
f_t	tyre force input (N)
k_s	suspension spring stiffness (N/m)
k_t	tyre spring stiffness (N/m)
m_s	sprung mass (kg)
$\hat{m}_s, \hat{m}_u, \ldots$	estimated values of parameters
m_u	unsprung mass (kg)
$\boldsymbol{q}$	variable to be removed after perturbation
$\mathbf{T}_b$	transformation matrix for balancing
$\mathbf{T}_m$	modal transformation matrix
u	control force input (N)
$\mathbf{W}$	Grammian matrix of balanced system
$\boldsymbol{x}$	state vector of original model
$\boldsymbol{x}_b$	state vector of balanced system
$\boldsymbol{x}_m$	state vector after modal transformation
$\boldsymbol{x}_r$	state vector of the reduced-order model
$\boldsymbol{x}_s$	state vector of two-mass model
$\boldsymbol{y}$	output vector
$z_i, \psi_i, \theta_i, \phi_i$	variables for suspension part i
z_s, z_u	displacement sprung mass and unsprung mass
Δ	characteristic polynomial
μ	very small parameter to be perturbed

The MS was received on 9 June 1999 and was accepted after revision for publication on 24 February 2000.
* *Corresponding author: Department of Mechanical and Aerospace Engineering, North Carolina State University, Box 7910, Raleigh, NC 27695-7910, USA.*

1 INTRODUCTION

Active control of vehicle suspension systems has been a topic of growing interest for years. The benefits of active suspension have been known as improved ride quality and handling performance at the same time, which are the trade-offs in conventional passive systems. As a result, there have been a great number of papers on this topic that explore various kinds of control algorithms [**1**–**4**].

In most cases, the quarter-car system in Fig. 1 is used for the ride analysis and active suspension design. With the current trend of four independent suspension systems on a single automobile, a quarter-car system

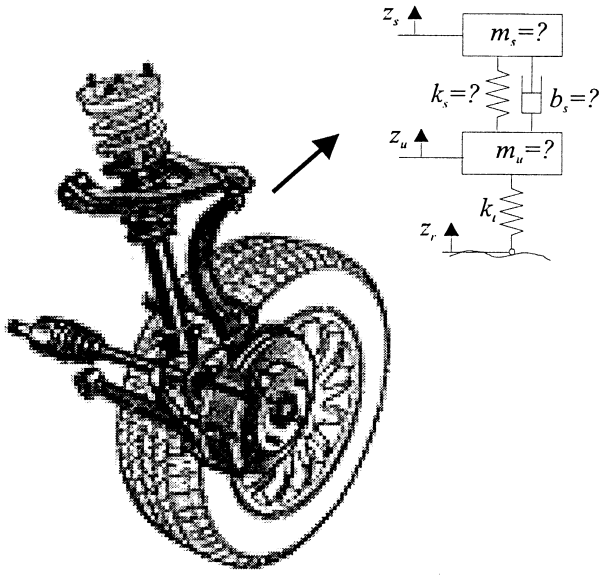

Fig. 1 A quarter-car suspension system and its simplified model (two-mass model)

offers a quite reasonable representation of the actual suspension system.

As a simplified model for the quarter-car system, a well-known two-mass model has been used mostly. The two-mass model is simple yet effective in representing the two dominant modes (sprung mass bouncing and wheel hopping) of a quarter-car system.

The two-mass model is composed of two lumped masses, a linear spring, a damper and a tyre. In many previous works, these data have been assumed to be available. For example, the spring stiffness and damping coefficient are obtained on the basis of component data. Also, the unsprung mass is calculated using the summation of suspension linkages. However, as shown in the previous study [**5**], the simple model may not be as effective as might be expected without considering the influence of the suspension kinematic structure. For example, two suspension systems with the same component properties behave differently with different suspension kinematic structures. As a suspension system becomes more complex (e.g. double wishbone type, multilink type, etc.), the suspension kinematic structure takes on a greater impact.

The study [**5**] shows that the response of two-mass model with the nominal set of data (based on the component data) is different from the response of the real system. A parameter identification method based on the least-squares method was used to obtain a more accurate set of equivalent parameters. It was observed that the values of the identified parameters varied widely depending on the suspension structure. Even for the same suspension type, different linkage layouts produced different sets of identified parameters.

With the parameter identification, the identified simple model becomes closer to the real system than the nominal simple model. However, there still exist some discrepancies between the identified simple model and the real system for the actuator input response. Finding possible sources of these discrepancies is the primary motivation of this present study.

The reason for the discrepancies could be one (or both) of the following: (a) the limitation of two-mass model structure; (b) the limitation of the least-squares method in approximating the parameters.

In order to investigate the first possibility, a real quarter system is modelled as a complex multibody dynamic system. The model includes all the suspension linkages and connecting elements (e.g. spring, damping, bushings and joints, etc.). As a result, the complex model has considerably more degrees of freedom (DOF) than the two-mass model.

After the complex model has been linearized, several model reduction techniques are used to find an 'optimal' reduced-order model (i.e. the smallest size model which is close to the real system). A classical dominant mode technique and the balanced realization technique are used. As a result, a reduced-order model which has the same size as the two-mass model is obtained.

For the second possibility, a more accurate set of equivalent parameters is obtained by comparing the reduced-order model and the two-mass model. The result reveals the effectiveness of the two-mass model structure, assuming that accurate equivalent parameters are used. In the process, a convenient way of obtaining the set of equivalent parameters of the two-mass system is introduced. Also, an experimental way of obtaining the equivalent parameters is described. Finally, the effect of suspension type on the equivalent parameters is investigated.

The rest of this paper is organized as follows. In Section 2, obtaining simple models using model reduction techniques is described. In Section 3, a set of equivalent parameters of a two-mass model is obtained by comparing the result of Section 2. In Section 4, an experimental way of finding equivalent parameters is proposed. In Section 5, the effect of suspension structure on the equivalent parameters is investigated for a different type of suspension system. The conclusion reviews and recommends further topics.

2 SIMPLIFIED MODEL USING MODEL REDUCTIONS

2.1 Suspension models for a quarter-car

Figure 2a shows a complex multibody dynamic model used to analyse a quarter-car system which includes suspension linkage and connecting elements (e.g. bushings, joints, . . . , etc.). With the help of commercial soft-

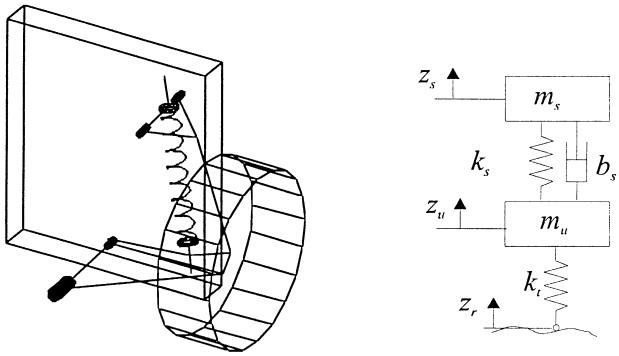

(a) a complex ADAMS model (b) simple two-mass model

Fig. 2 Models of a quarter-car suspension system

ware it becomes easy to build such a complex system and to obtain an accurate system response.

So far, however, a simple two-mass model (Fig. 2b) has been used the most frequently in the field of active suspension studies. This is because the model is simple yet captures important characteristics of a real vehicle including two major vibration modes (bouncing and wheel hopping). The two-mass model is composed of the sprung mass and the unsprung mass connected with spring and damping elements. The tyre is modelled as a linear spring and its damping is neglected in many cases. The key to modelling a quarter-car system with a two-mass model structure is determining these equivalent parameters (m_s, m_u, k_s, b_s and k_t).

In much on-going research on active suspension, the equivalent parameters are assumed to be known. Mostly, the parameters are obtained from the component data provided by suspension part vendors. This is especially true for the spring, tyre and damper elements. The unsprung mass is usually calculated from the summation of suspension links which move along with the wheel and tyre. Finally, the sprung mass is calculated by subtracting the unsprung mass from the entire quarter car load.

However, the 'nominal model' (a model that is based on component data) may not be as effective as might be expected. As shown in the previous study **[5]**, there exist 'invisible uncertainties' (i.e. those that are not shown in the component data) owing to its suspension structure. That is, the equivalent suspension parameters of the simple model are highly affected by the change of suspension linkage layout and/or structure. Figure 3 shows the discrepancies between the responses of the original system and the simple model with nominal data.

If the discrepancy comes from the limitation of model structure, then it raises a question, 'What is the smallest size of model that describes the real quarter car system with reasonable accuracy?' In order to answer the question, the present work starts with the complex model of Fig. 2a.

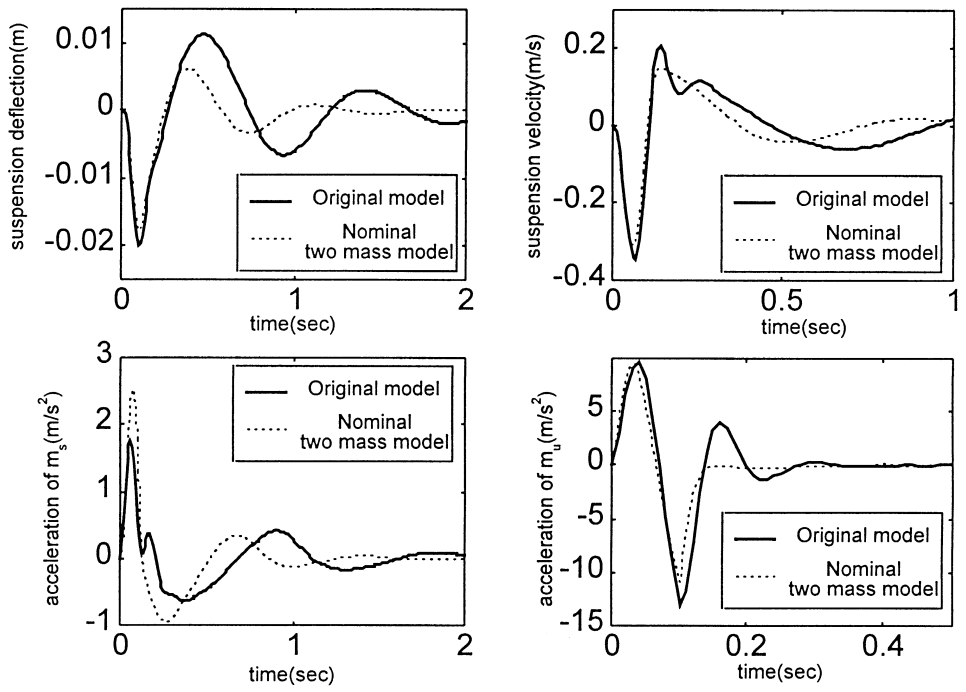

Fig. 3 The comparison of the system responses between the original system and the nominal simple model. (From reference **[5]**)

Table 1 The definitions of variable and body numbers

Variables	Definition	Number of body	Name of body
$\dot{z}, z$	Vertical displacement and velocity	1	Car body (sprung mass)
$\dot{\psi}, \psi$	Yaw rate and yaw angle	2	Upper control arm
$\dot{\theta}, \theta$	Pitch rate and pitch angle	3	Lower control arm
$\dot{\phi}, \phi$	Roll rate and roll angle	4	Knuckle and wheel
		5	Tie rod
		6	Road excitor
		7	Strut upper part
		8	Strut lower part

2.2 Linearization of a complex suspension model

A complex ADAMS model (Fig. 2a) is described by a set of non-linear equations of motion:

$$\dot{\boldsymbol{x}} = \boldsymbol{f}(\boldsymbol{x}, u, f_t) \tag{1a}$$

$$\boldsymbol{y} = \boldsymbol{g}(\boldsymbol{x}) \tag{1b}$$

where $\boldsymbol{x}$, u and f_t are system state vector, control input and tyre force input respectively.

Linearizing the equations around an equilibrium position and using $f_t = k_t w$ for tyre force, large-order linearized equations of motion can be obtained:

$$\dot{\boldsymbol{x}} = \mathbf{A}\boldsymbol{x} + \mathbf{B}u + \mathbf{G}w \tag{2a}$$

$$\boldsymbol{y} = \mathbf{C}\boldsymbol{x} \tag{2b}$$

where

$$\mathbf{A} = \frac{\partial \boldsymbol{f}}{\partial \boldsymbol{x}} \in \Re^{32\times 32}, \qquad \mathbf{B} = \frac{\partial \boldsymbol{f}}{\partial u} \in \Re^{32\times 1}$$

$$\mathbf{G} = k_t \frac{\partial \boldsymbol{f}}{\partial f_t} \in \Re^{32\times 1}, \qquad \mathbf{C} = \frac{\partial \boldsymbol{g}}{\partial \boldsymbol{x}} \in \Re^{4\times 32}$$

and k_t is the tyre stiffness and w is the road displacement input.

The control input u is the force generated by the actuator installed parallel to the strut. The system output $\boldsymbol{y}$ is defined as a 4×1 vector of displacement and velocity of car body and wheel. For the double wishbone type suspension model in Fig. 2a, the system has 16 DOF. The corresponding states of the linearized equations of motion are composed of 32 states:

$$\begin{aligned}\boldsymbol{x} = [&\dot{z}_1 \;\; z_1 \;\; \dot{\psi}_2 \;\; \psi_2 \;\; \dot{\phi}_2 \;\; \phi_2 \;\; \dot{\theta}_2 \;\; \theta_2 \;\; \dot{\psi}_3 \;\; \psi_3 \;\; \dot{\phi}_3 \;\; \phi_3 \cdots \\ &\dot{\theta}_3 \;\; \theta_3 \;\; \dot{\psi}_4 \;\; \psi_4 \;\; \dot{\phi}_4 \;\; \phi_4 \;\; \dot{\theta}_4 \;\; \theta_4 \;\; \dot{\psi}_5 \;\; \psi_5 \\ &\dot{\phi}_5 \;\; \phi_5 \;\; \dot{z}_7 \;\; z_7 \;\; \dot{\phi}_7 \;\; \phi_7 \;\; \dot{\theta}_7 \;\; \theta_7 \;\; \dot{\psi}_8 \;\; \psi_8]\end{aligned} \tag{3}$$

$$\boldsymbol{y} = [z_1 \;\; \dot{z}_1 \;\; z_4 \;\; \dot{z}_4]^{\mathrm{T}} = \mathbf{C}\boldsymbol{x} \tag{4}$$

The definitions of variables and body numbers are shown in Table 1. The subscript of each variable represents the number of body used in the ADAMS model.

Figure 4 shows the comparison of the response of the linearized model and the original ADAMS complex system. The result shows that there is little difference between the responses before and after the linearization. Even if the difference may become larger for a higher amplitude input, 0.025 m road input is fairly acceptable as the nominal range of road input [**3**]. Therefore, it can be concluded that the linearized model is very close to the original system.

2.3 Model reduction of a quarter-car suspension model

From the perspective of controller design, the large-order linearized model of equations (2) has little practical use unless it is reduced to a manageable size without sacrificing accuracy.

Model order reduction has been a major topic in systems theory for decades. Various kinds of techniques have been developed since it first appeared in the late 1960s [**6–8**]. Pade approximation, modal approximation and continued fraction expansions were the typical methodologies in the beginning. Singular perturbation was also applied to model reduction [**9**]. Singular perturbation is very similar to the dominant mode technique in the sense of separating the modes based on their 'fastness' [**9**]. The balanced realization technique is applied to the model reduction by Moore [**10**]. The method is based on measures of controllability and observability of the system. The most controllable and observable portion of the dynamics is used as a low-order approximation for the model. In this section, three different kinds of model techniques are applied to the quarter-car with a brief review of each method.

2.3.1 Reduced-order model using a dominant mode technique (model I)

To the linearized model of equations (2), a modal transformation (using $\boldsymbol{x} = \mathbf{T}_m \boldsymbol{z}_m$) can be applied to

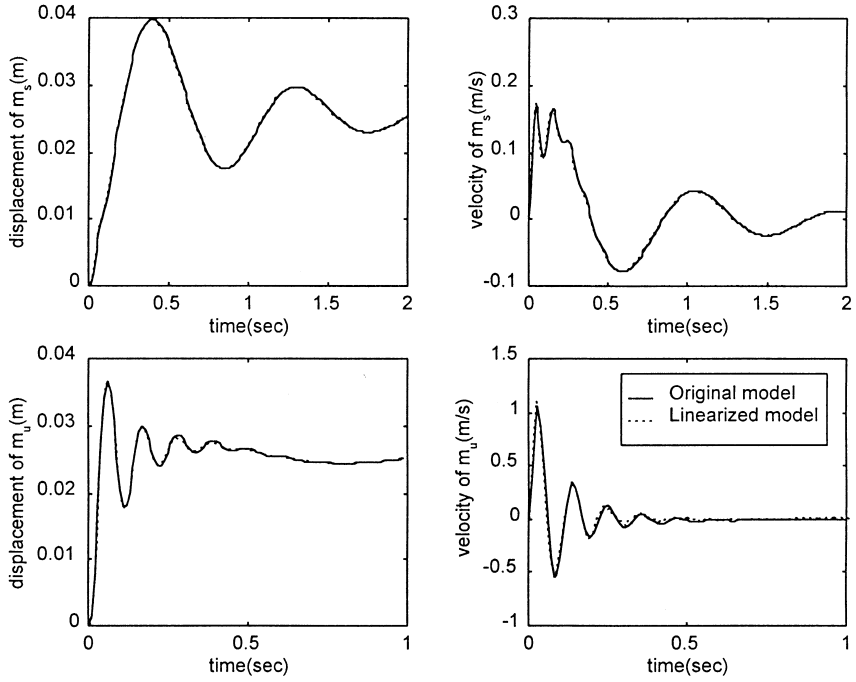

Fig. 4 The comparison of road input responses (original model and its linearized model)

obtain a decoupled modal state space equation.

$$\dot{z}_m = \mathbf{T}_m^{-1}\mathbf{A}\mathbf{T}_m z_m + \mathbf{T}_m^{-1}\mathbf{B}u + \mathbf{T}_m^{-1}\mathbf{G}w$$
$$= \mathbf{A}_m z_m + \mathbf{B}_m u + \mathbf{G}_m w \quad (5a)$$
$$y = \mathbf{C}\mathbf{T}_m z_m = \mathbf{C}_m z_m \quad (5b)$$

where

$$\mathbf{A}_m = \begin{bmatrix} \mathbf{A}_{m11} & \mathbf{A}_{m12} \\ \mathbf{A}_{m21} & \mathbf{A}_{m22} \end{bmatrix}, \qquad \mathbf{B}_m = \begin{bmatrix} \mathbf{B}_{m1} \\ \mathbf{B}_{m2} \end{bmatrix}$$
$$\mathbf{G}_m = \begin{bmatrix} \mathbf{G}_{m1} \\ \mathbf{G}_{m2} \end{bmatrix}, \qquad \mathbf{C}_m = [\mathbf{C}_{m1} \quad \mathbf{C}_{m2}]$$

Each block matrix is divided into slow modes and fast modes based on the magnitudes of eigenvalues. Then, the following reduced-order linear system ($m \times m$) is obtained by neglecting the fast modes:

$$\dot{z}_r = \mathbf{A}_r z_r + \mathbf{B}_r u + \mathbf{G}_r w$$
$$= \mathbf{A}_{m11} z_r + \mathbf{B}_{m1} u + \mathbf{G}_{m1} w \quad (6a)$$
$$y = \mathbf{C}_r z_r = \mathbf{C}_{m1} z_r \quad (6b)$$

where

$$z_r \in \Re^{m\times 1}$$

By eliminating the least dominant modes (with the biggest eigenvalues) one by one, a reduced-order model (model I) with four states can be obtained as follows. When m is smaller than 4, there is a significant difference between the responses of the two systems [i.e. Equations (2b) and (6b)]. The process results in the following system matrices:

$$\mathbf{A}_r = \begin{bmatrix} -1.3438 \times 10^0 & 6.9834 \times 10^0 & 0 & 0 \\ -6.9834 \times 10^0 & -1.3438 \times 10^0 & 0 & 0 \\ 0 & 0 & -8.4582 \times 10^0 & 5.1584 \times 10^1 \\ 0 & 0 & -5.1584 \times 10^1 & -8.4582 \times 10^0 \end{bmatrix}$$

$$\mathbf{B}_r = \begin{bmatrix} -9.2749 \times 10^{-3} \\ -2.2295 \times 10^{-3} \\ +5.3175 \times 10^{-2} \\ -2.6143 \times 10^{-2} \end{bmatrix}, \qquad \mathbf{G}_r = \begin{bmatrix} -3.1578 \times 10^2 \\ 6.2705 \times 10^1 \\ -1.5590 \times 10^4 \\ 6.7116 \times 10^3 \end{bmatrix}$$

and

$$\mathbf{C}_{\mathrm{r}} = \begin{bmatrix} -4.0800 \times 10^{-3} & 2.0760 \times 10^{-2} \\ -1.3949 \times 10^{-1} & -5.6389 \times 10^{-2} \\ -1.3179 \times 10^{-3} & 2.0221 \times 10^{-3} \\ -1.2350 \times 10^{-2} & -1.1921 \times 10^{-2} \end{bmatrix}$$

$$\begin{bmatrix} 2.2538 \times 10^{-4} & 1.4005 \times 10^{-4} \\ -9.1307 \times 10^{-3} & 1.0441 \times 10^{-2} \\ 1.1612 \times 10^{-3} & 2.5770 \times 10^{-3} \\ -1.4275 \times 10^{-1} & 3.8102 \times 10^{-2} \end{bmatrix}$$

The eigenvalues of the reduced-order system are as follows:

$$\lambda_{1,2} = -1.3438 \pm \mathrm{j}6.9834 \quad (\rightarrow f_{\mathrm{n}} = 1.1318 \text{ Hz})$$

$$\lambda_{3,4} = -8.4582 \pm \mathrm{j}51.584 \quad (\rightarrow f_{\mathrm{n}} = 8.3194 \text{ Hz})$$

Figure 5 shows the corresponding two modes of the reduced-order model, which clearly reflect body bouncing and wheel hopping.

2.3.2 *Reduced-order model using balanced realization technique (model II)*

From equation (2), a 'balanced' system is obtained using a similarity transformation $\boldsymbol{z}_{\mathrm{b}} = \mathbf{T}_{\mathrm{b}}\boldsymbol{x}$:

$$\dot{\boldsymbol{z}}_{\mathrm{b}} = \mathbf{T}_{\mathrm{b}}\mathbf{A}\mathbf{T}_{\mathrm{b}}^{-1}\boldsymbol{z}_{\mathrm{b}} + \mathbf{T}_{\mathrm{b}}\mathbf{B}u + \mathbf{T}_{\mathrm{b}}\mathbf{G}w$$

$$= \mathbf{A}_{\mathrm{b}}\boldsymbol{z}_{\mathrm{b}} + \mathbf{B}_{\mathrm{b}}u + \mathbf{G}_{\mathrm{b}}w \tag{7a}$$

$$\boldsymbol{y} = \mathbf{C}\mathbf{T}_{\mathrm{b}}^{-1}\boldsymbol{z}_{\mathrm{b}} = \mathbf{C}_{\mathrm{b}}\boldsymbol{z}_{\mathrm{b}} \tag{7b}$$

For the balanced system, the Grammian matrix, $\mathbf{W}$, satisfies the Lyapunov equations, i.e.

$$\mathbf{W}\mathbf{A}_{\mathrm{b}}^{\mathrm{T}} + \mathbf{A}_{\mathrm{b}}\mathbf{W} = -\mathbf{B}_{b}\mathbf{B}_{\mathrm{b}}^{\mathrm{T}} \tag{8a}$$

$$\mathbf{W}\mathbf{A}_{\mathrm{b}} + \mathbf{A}_{\mathrm{b}}^{\mathrm{T}}\mathbf{W} = -\mathbf{C}_{b}^{\mathrm{T}}\mathbf{C}_{\mathrm{b}} \tag{8b}$$

Equations (8) mean that the relationships from input to states and from states to output are internally balanced.

Here, the 'dominance' of a state is determined by the singular values of the Grammian matrix of the balanced system. Figure 6 shows its distribution for the balanced

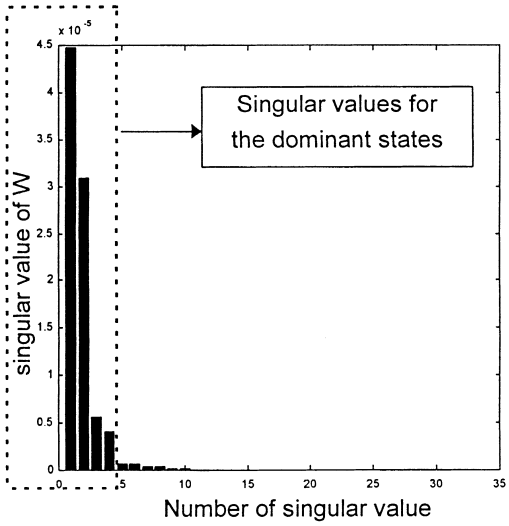

Fig. 6 The distribution of the singular values of W for the balanced system

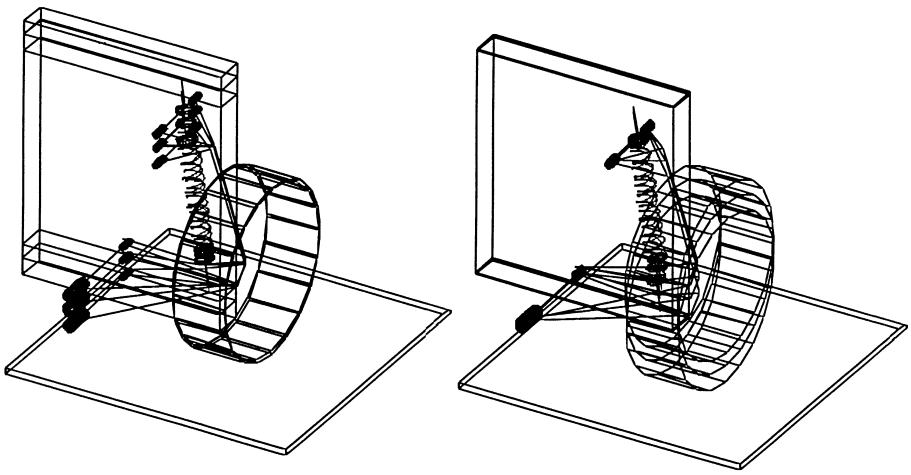

(a) Mode 1 at frequency =1.13 Hz (b) Mode 2 at frequency = 8.30 Hz

Fig. 5 Two mode shapes remaining in the reduced-order model

system. Each matrix is divided into the dominant and non-dominant states as follows:

$$\mathbf{A}_b = \begin{bmatrix} \mathbf{A}_{b11} & \mathbf{A}_{b12} \\ \mathbf{A}_{b21} & \mathbf{A}_{b22} \end{bmatrix}, \qquad \mathbf{B}_b = \begin{bmatrix} \mathbf{B}_{b1} \\ \mathbf{B}_{b2} \end{bmatrix}$$

$$\mathbf{G}_b = \begin{bmatrix} \mathbf{G}_{b1} \\ \mathbf{G}_{b2} \end{bmatrix}, \qquad \mathbf{C}_b = [\mathbf{C}_{b1} \quad \mathbf{C}_{b2}]$$

Then, the following 4×4 reduced-order linear system (model II) is obtained by neglecting the non-dominant states one by one until there is marked difference of responses between the two systems:

$$\dot{\boldsymbol{z}}_r = \mathbf{A}_r \boldsymbol{z}_r + \mathbf{B}_r u + \mathbf{G}_r w = \mathbf{A}_{b11} \boldsymbol{z}_r + \mathbf{B}_{b1} u + \mathbf{G}_{b1} w \tag{9a}$$

$$\boldsymbol{y} = \mathbf{C}_r \boldsymbol{z}_r = \mathbf{C}_{b1} \boldsymbol{z}_r \tag{9b}$$

where

$$\boldsymbol{z}_r \in \Re^{m \times 1}$$

The numerical results are

$$\mathbf{A}_r = \begin{bmatrix} -1.0161 \times 10^0 & 7.0313 \times 10^0 & 3.3967 \times 10^{-1} & 2.2935 \times 10^{-1} \\ -7.0364 \times 10^0 & -1.6972 \times 10^0 & 1.0831 \times 10^{-1} & -1.3293 \times 10^0 \\ -1.8690 \times 10^0 & -2.8603 \times 10^0 & -6.5056 \times 10^0 & -5.1431 \times 10^1 \\ 1.9409 \times 10^0 & 3.2291 \times 10^0 & 5.1524 \times 10^1 & -1.0287 \times 10^1 \end{bmatrix}$$

$$\mathbf{B}_r = \begin{bmatrix} 9.5305 \times 10^{-3} \\ 1.0234 \times 10^{-2} \\ 8.5643 \times 10^{-3} \\ -9.2014 \times 10^{-3} \end{bmatrix}, \qquad \mathbf{G}_r = \begin{bmatrix} 4.8671 \times 10^2 \\ 1.0913 \times 10^2 \\ -2.6819 \times 10^3 \\ 2.5163 \times 10^3 \end{bmatrix}$$

and

$$\mathbf{C}_r = \begin{bmatrix} 9.5029 \times 10^{-3} & -1.0094 \times 10^{-2} & 1.6416 \times 10^{-4} & -1.2237 \times 10^{-3} \\ 5.8675 \times 10^{-2} & 7.9504 \times 10^{-2} & -6.1832 \times 10^{-2} & 2.0441 \times 10^{-2} \\ 7.2478 \times 10^{-4} & -1.6863 \times 10^{-3} & -8.5627 \times 10^{-3} & -9.1197 \times 10^{-3} \\ 9.4795 \times 10^{-3} & 3.0739 \times 10^{-3} & -4.1597 \times 10^{-1} & 5.3181 \times 10^{-1} \end{bmatrix}$$

2.3.3 *Reduced-order model using singular perturbation (model III)*

In order to fit the steady states of the original system and the reduced-order system, the following correction using the singular perturbation technique is added.

By introducing a small parameter, μ, to the second part (non-dominant portion) of the system equation, the system equations are changed to

$$\begin{Bmatrix} \dot{\boldsymbol{x}}_r \\ \mu \dot{\boldsymbol{q}} \end{Bmatrix} = \begin{bmatrix} \mathbf{A}_{11} & \mathbf{A}_{12} \\ \mathbf{A}_{21} & \mathbf{A}_{22} \end{bmatrix} \begin{Bmatrix} \dot{\boldsymbol{x}}_r \\ \mu \dot{\boldsymbol{q}} \end{Bmatrix} + \begin{bmatrix} \mathbf{B}_1 \\ \mathbf{B}_2 \end{bmatrix} u + \begin{bmatrix} \mathbf{G}_1 \\ \mathbf{G}_2 \end{bmatrix} w \tag{10}$$

where

$\boldsymbol{x}_r \in \Re^m$ is the state vector of the dominant portion
$\boldsymbol{q} \in \Re^{n-m}$ is the state vector of the non-dominant portion

By giving a perturbation $\mu \to 0$, the system order drops to m. Then, the second part of Equation (10) becomes the steady state relationship between $\boldsymbol{x}_r$ and $\mathbf{q}$. Finally, using the algebraic relationship, the first part of the differential equation (10) becomes a reduced-order system:

$$\dot{\boldsymbol{z}}_r = \mathbf{A}_r \boldsymbol{z}_r + \mathbf{B}_r u + \mathbf{G}_r w \tag{11a}$$

$$\boldsymbol{y} = \mathbf{C}_r \boldsymbol{z}_r + \mathbf{D}_r u + \mathbf{E}_r w \tag{11b}$$

where

$$\mathbf{A}_r = \mathbf{A}_{11} - \mathbf{A}_{12}\mathbf{A}_{22}^{-1}\mathbf{A}_{21}, \qquad \mathbf{B}_r = \mathbf{B}_1 - \mathbf{A}_{12}\mathbf{A}_{22}^{-1}\mathbf{B}_2$$

$$\mathbf{G}_r = \mathbf{G}_1 - \mathbf{A}_{12}\mathbf{A}_{22}^{-1}\mathbf{G}_2$$

$$\mathbf{C}_r = \mathbf{C}_1 - \mathbf{C}_2\mathbf{A}_{22}^{-1}\mathbf{A}_{21}, \qquad \mathbf{D}_r = -\mathbf{C}_2\mathbf{A}_{22}^{-1}\mathbf{B}_2$$

$$\mathbf{E}_r = -\mathbf{C}_2\mathbf{A}_{22}^{-1}\mathbf{G}_2$$

If the technique is applied to the balanced system, the following reduced-order model is obtained. Notice that

two non-zero matrices, $\mathbf{D}_r$ and $\mathbf{E}_r$, show the effect of inputs on the output states:

$$\mathbf{A}_r = \begin{bmatrix} -1.0161 \times 10^0 & 7.0313 \times 10^0 \\ -7.0363 \times 10^0 & -1.6970 \times 10^0 \\ -1.8596 \times 10^0 & -2.8457 \times 10^0 \\ 1.9545 \times 10^0 & 3.2502 \times 10^0 \end{bmatrix}$$

$$\begin{bmatrix} 3.3992 \times 10^{-1} & 2.2900 \times 10^{-1} \\ 1.0918 \times 10^{-1} & -1.3308 \times 10^0 \\ -6.4392 \times 10^0 & -5.1531 \times 10^1 \\ 5.1623 \times 10^1 & -1.0430 \times 10^1 \end{bmatrix}$$

$$\mathbf{B}_r = \begin{bmatrix} 9.5303 \times 10^{-3} \\ 1.0234 \times 10^{-2} \\ 8.5205 \times 10^{-3} \\ -9.26541 \times 10^{-3} \end{bmatrix}, \quad \mathbf{G}_r = \begin{bmatrix} 4.8672 \times 10^2 \\ 1.0930 \times 10^2 \\ -2.6724 \times 10^3 \\ 2.5303 \times 10^3 \end{bmatrix}$$

$$\mathbf{C}_r = \begin{bmatrix} 9.5023 \times 10^{-3} & -1.0095 \times 10^{-2} \\ 5.8675 \times 10^{-2} & 7.9504 \times 10^{-2} \\ 7.3088 \times 10^{-4} & -1.6768 \times 10^{-3} \\ 9.2282 \times 10^{-3} & 2.6840 \times 10^{-3} \end{bmatrix}$$

$$\begin{bmatrix} 1.5961 \times 10^{-4} & -1.2171 \times 10^{-3} \\ -6.2100 \times 10^{-2} & 1.9913 \times 10^{-2} \\ -8.5190 \times 10^{-3} & -9.1848 \times 10^{-3} \\ -4.1558 \times 10^{-1} & 5.3877 \times 10^{-1} \end{bmatrix}$$

and

$$\mathbf{D}_r = \begin{bmatrix} 2.9348 \times 10^{-9} \\ -3.8509 \times 10^{-10} \\ -2.8622 \times 10^{-8} \\ 1.1870 \times 10^{-6} \end{bmatrix}, \quad \mathbf{E}_r = \begin{bmatrix} -5.3280 \times 10^{-4} \\ -1.2952 \times 10^{-2} \\ 6.2526 \times 10^{-3} \\ -2.4063 \times 10^{-2} \end{bmatrix}$$

2.3.4 *Comparison*

In order to compare the results using these techniques, eigenvalues of the reduced-order models are listed in Table 2. The results show that there is no significant difference among all three techniques. However, this is not always true for the general case. In this specific case for the quarter-car system, the dominant mode (based on eigenvalues) coincides with the most controllable and observable states.

Figures 7 and 8 show the comparisons of the original system and the reduced system for actuator input and road displacement input. Since it is hard to distinguish three reduced-order models, there is only one reduced-order model (model II) shown in the figures. On the basis of the results, it can be said that the reduced-order model with four states represents the original system with considerable accuracy for both control input and road displacement input.

3 EQUIVALENT PARAMETERS FOR TWO-MASS MODEL

From the result of Section 2, it is observed that the size of the reduced-order model is as small as that of the two-mass model with no apparent sacrifice in accuracy. In this section, the relationship between the reduced-order model and the two-mass model is investigated. The goal is to obtain a set of equivalent parameters for the two-mass model such that its response is as close to the reduced-order model as possible. In this way, the effectiveness of the two-mass model structure can be verified.

The system matrices of the two-mass model are

$$\dot{\boldsymbol{x}} = \mathbf{A}\boldsymbol{x} + \mathbf{B}u + \mathbf{G}w \tag{12}$$

Table 2 Eigenvalues of reduced-order models using three different model reductions

	Model I	Model II	Model III
$\lambda_{1,2}$ (f_n (Hz))	$-1.3438 \pm j6.9834$ (1.1318)	$-1.3436 \pm j6.9834$ (1.1318)	$-1.3438 \pm j6.9834$ (1.1318)
$\lambda_{3,4}$ (f_n (Hz))	-8.4582 ± 51.584 (8.3194)	-8.4092 ± 51.497 (8.3045)	-8.4472 ± 51.593 (8.3205)

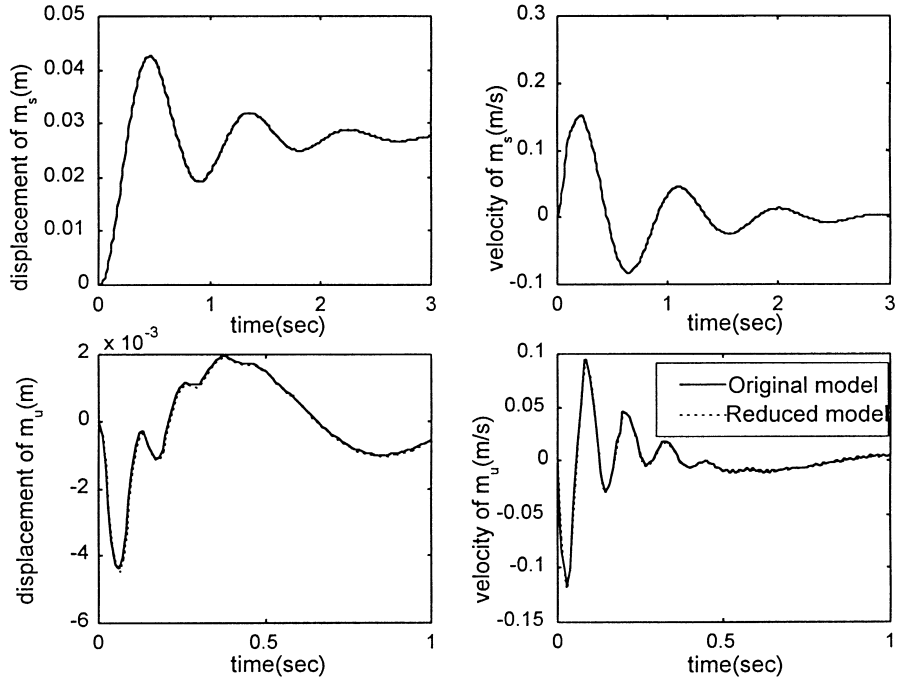

Fig. 7 The comparison of actuator input responses (original model and reduced-order model)

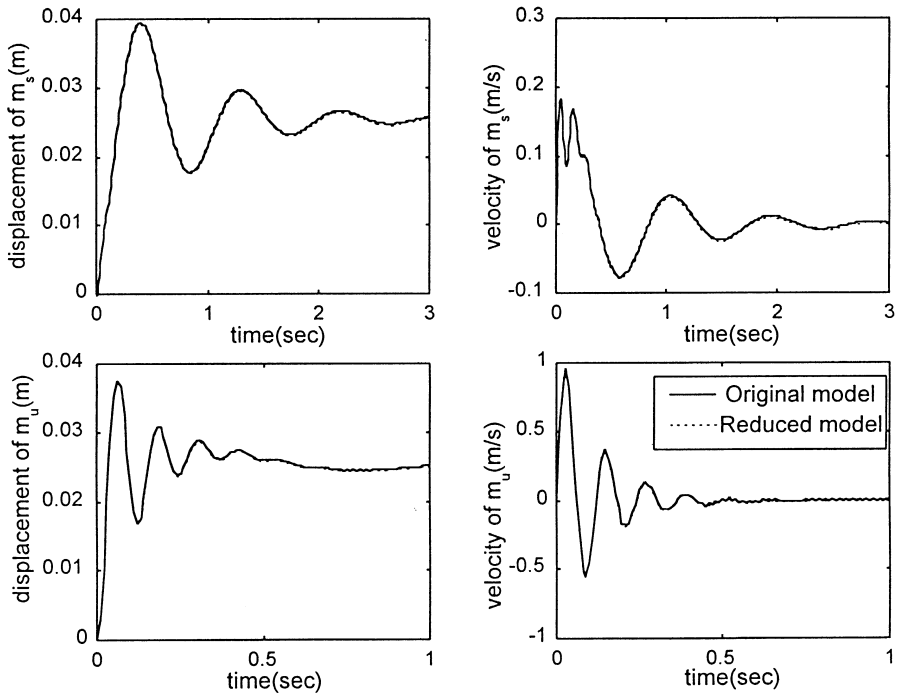

Fig. 8 The comparison of road input responses (original model and reduced-order model)

where

$$\boldsymbol{x} = [z_s \;\; \dot{z}_s \;\; z_u \;\; \dot{z}_u]^T$$

$$\mathbf{A} = \begin{bmatrix} 0 & 1 & 0 & 0 \\ -k_s/m_s & -b_s/m_s & k_s/m_s & b_s/m_s \\ 0 & 0 & 0 & 1 \\ k_s/m_u & b_s/m_u & -(k_s+k_t)/m_u & -b_s/m_u \end{bmatrix}$$

$$\mathbf{B} = \begin{bmatrix} 0 \\ 1/m_s \\ 0 \\ -1/m_u \end{bmatrix}, \qquad \mathbf{G} = \begin{bmatrix} 0 \\ 0 \\ 0 \\ k_t/m_u \end{bmatrix}$$

In order to express the reduced-order model with the same state vector, another similarity transformation is applied to the model. Using $\boldsymbol{x} = \mathbf{C}_r\mathbf{z}_r$, equation (12) becomes

$$\begin{aligned} \dot{\boldsymbol{x}} &= \mathbf{C}_r\mathbf{A}_r\mathbf{C}_r^{-1}\boldsymbol{x} + \mathbf{C}_r\mathbf{B}_r u + \mathbf{C}_r\mathbf{G}_r w \\ &= \bar{\mathbf{A}}_r\boldsymbol{x} + \bar{\mathbf{B}}_r u + \bar{\mathbf{g}}_r w \end{aligned} \tag{13}$$

In the case of model I, the transformation results in

$$\bar{\mathbf{A}}_r = \begin{bmatrix} 0 & 1 & 0 & 0 \\ -2.3609 \times 10^1 & -1.4383 \times 10^0 & -2.3255 \times 10^2 & 1.4240 \times 10^0 \\ 0 & 0 & 0 & 1 \\ 3.0609 \times 10^2 & 1.7931 \times 10^1 & -2.7796 \times 10^3 & -1.7713 \times 10^1 \end{bmatrix}$$

$$\bar{\mathbf{B}}_r = \begin{bmatrix} 0 \\ 6.5522 \times 10^{-4} \\ 0 \\ -8.3341 \times 10^{-3} \end{bmatrix}, \qquad \bar{\mathbf{G}}_r = \begin{bmatrix} 4.1764 \times 10^{-3} \\ 2.5450 \times 10^2 \\ 1.8551 \times 10^{-1} \\ 2.4587 \times 10^3 \end{bmatrix}$$

The reduced-order model includes the effect of suspension geometric characteristics (e.g. the lengths of links, etc.) while the two-mass model does not. Therefore, the difference of the model structures for the two systems is not surprising. Notice that the simple relationships among the elements of $\mathbf{A}$ do not hold for $\bar{\mathbf{A}}_r$. For example, $\bar{\mathbf{A}}_r(2,2)$ is not equal to $-\bar{\mathbf{A}}(2,4)$ while $\mathbf{A}(2,4)$ is equal to $-\mathbf{A}(2,2)$. Therefore, it is not easy to obtain equivalent parameters by matching the system matrices of reduced-order system and two-mass model element by element. There can be many different results of parameter estimation depending on the choice of elements. Instead, a comparison of the characteristic equations of two systems is used to obtain the equivalent parameters in the present study.

From the equation of motion for the two-mass system, the transfer function from the actuator control force, u , to the suspension deflection, $z_s - z_u$, is derived as

$$\frac{z_s(s) - z_u(s)}{u(s)} = \frac{(m_s + m_u)s^2/m_s m_u + k_t/(m_s m_u)}{\Delta} \tag{14}$$

where Δ is the characteristic polynomial

$$\Delta = s^4 + \left(\frac{m_s + m_u}{m_s m_u}\, b_s\right)s^3 + \frac{m_s(k_s + k_t) + m_u k_s}{m_s m_u}\, s^2 + \frac{b_s k_t}{m_s m_u}\, s + \frac{k_s k_t}{m_s m_u} \tag{15}$$

The same transfer function for the reduced-order model is calculated using the result of Section 2.3:

$$\frac{z_s - z_u}{u} = \frac{b_2 s^2 + b_1 s + b_0}{s^4 + a_3 s^3 + a_2 s^2 + a_1 s + a_0} \tag{16}$$

where, the coefficients of the transfer function for three different reduced-order models are given in Table 3:

By matching the coefficients of the two transfer functions, an algorithm is developed to calculate a set of equivalent parameters (see Appendix for more detail):

$$\hat{k}_s = a_0/b_0 \tag{17a}$$

$$\hat{b}_s = a_1/b_0 \tag{17b}$$

$$\hat{m}_s = [a_2 - (a_3/\hat{b}_s)/\hat{k}_s]/b_0 \tag{17c}$$

$$\hat{m}_u = 1/(a_3/\hat{b}_s - 1/\hat{m}_s) \tag{17d}$$

$$\hat{k}_1 = b_0\hat{m}_s\hat{m}_u \tag{17e}$$

Using the algorithm, equivalent parameters for three reduced-order models are obtained (Table 4). As can be expected, the three models produced similar results since their characteristic equations are almost the same. Notice

Table 3 The coefficients of the transfer function for different reduced-order models

Coefficients	Model I (modal tech)	Model II (bal + del)	Model III (bal + mdc)
a_3	1.9604×10^1	1.9506×10^1	1.9582×10^1
a_2	2.8284×10^3	2.8184×10^3	2.8291×10^3
a_1	8.1991×10^3	8.1670×10^3	8.2000×10^3
a_0	1.3819×10^5	1.3769×10^5	1.3823×10^5
b_2	9.0634×10^{-3}	9.0183×10^{-3}	9.0533×10^{-3}
b_1	-8.7859×10^{-4}	-3.8264×10^{-4}	-9.5776×10^{-4}
b_0	3.7822	3.7676	3.7823

Table 4 Equivalent parameters for different reduced-order models

Estimated parameters	Model I	Model II	Model III	Component data
$\hat{k}_s$ (N/m)	36 537	36 546	36 543	37 278
$\hat{b}_s$ (N s/m)	2167.8	2167.7	2167.9	3000
$\hat{m}_s$ (kg)	660.48	660.78	660.68	404
$\hat{m}_u$ (kg)	132.82	133.60	132.99	45.24
$\hat{k}_t$ (N/m)	331 790	332 610	332 350	186 390

that some identified parameters are very far from the component data (e.g. $\hat{m}_s$, $\hat{m}_u$ and $\hat{k}_t$). The discrepancies between the component data and the identified parameters clearly show the possible inaccuracy of the nominal simple model. In other words, the nominal model without considering the suspension geometric structure has 'invisible' parameter uncertainties.

System responses of the two-mass model with the identified parameters are compared with the ones of the reduced-order model in Figs 9 and 10. The results show that there is little difference between two responses. From the results, it is pointed out that the model structure of the two-mass model is sufficiently effective to represent the quarter-car system. However, determining an accurate set of parameters is very crucial.

4 EXPERIMENTAL WAY OF OBTAINING EQUIVALENT PARAMETERS

In Section 3, the transfer function from the control input to the suspension deflection was calculated from the reduced-order model. Notice that the transfer function can also be obtained from the experimental set-up using a system identification method. That is, coefficients of the same transfer function are obtained using two sets of measured signals. Then, equations (17) can be used to obtain the set of equivalent parameters.

This process is very important considering that not all suspension component data are available to build a complex multibody dynamic model. Without an accurate complex model, needless to say, it is very difficult to obtain an accurate reduced-order model.

In order to demonstrate the feasibility of this approach, the original ADAMS model is used to generate two signals for the system identification. The suspension deflection response from the control force input is shown in Fig. 11.

Using the ARX function in MATLAB, the following transfer function with order 4 is obtained:

$$\frac{z_s - z_u}{u} = \frac{5.6539 \times 10^{-6} s^2 + 3.7693}{s^4 + 1.9517 \times 10^1 s^3 + 2.8196 \times 10^3 s^2 + 8.1708 \times 10^3 s + 1.3775 \times 10^5} \tag{18}$$

Figure 12 shows the comparison of the responses between the original and the identified model.

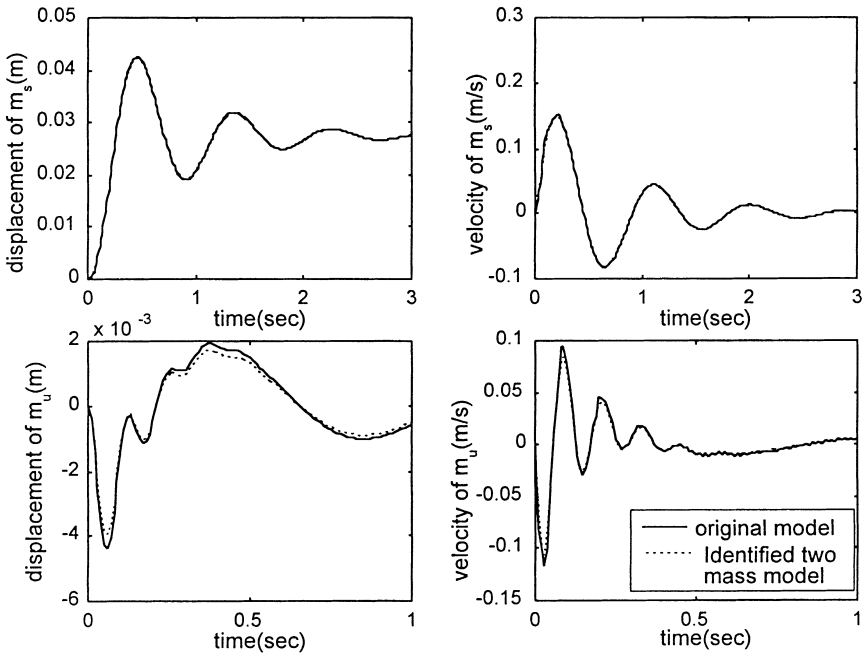

Fig. 9 The comparison of actuator input responses (original model versus identified two-mass model)

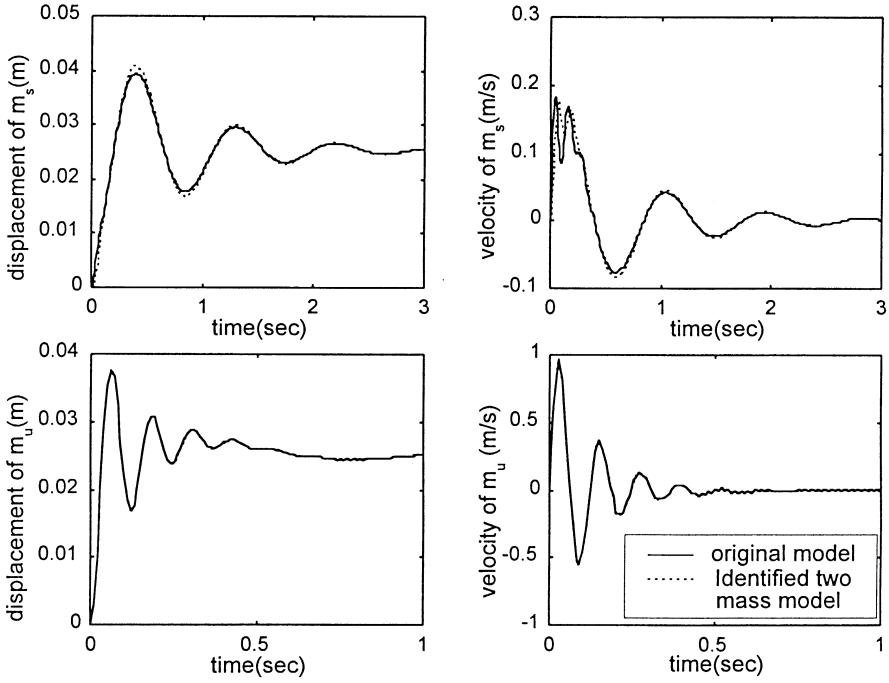

Fig. 10 The comparison of road input responses (original model versus identified two-mass model)

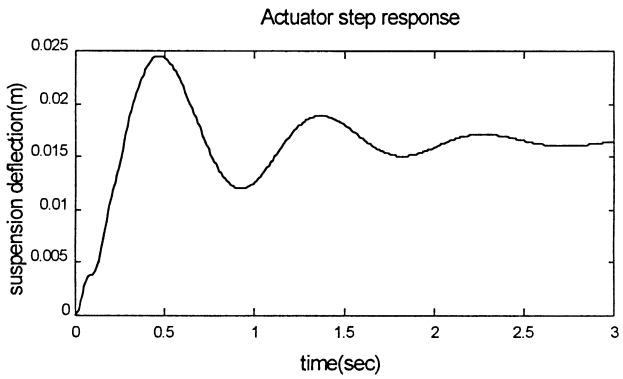

Fig. 11 Suspension deflection signal ($z_s - z_u$) from the actuator step response of the original system

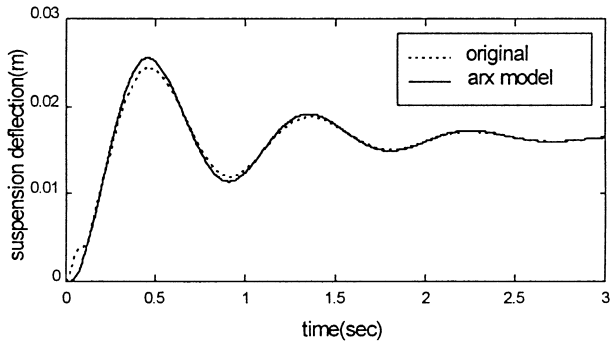

Fig. 12 The comparison of responses of the original system and identified (ARX) model

Notice that there are no real differences in the coefficients of the transfer function compared with the one in equation (16). The only difference is in the second-order term, b_2, in the numerator, which makes the difference in the responses in Fig. 12.

Using equation (18), similar results for identified parameters can be obtained. Table 5 shows the comparison of identified parameters with the reduced-order model and ARX model. The results show that the experimental way produces very accurate equivalent parameters for the two-mass model.

Figure 13 shows the actuator step responses for three different systems (the original system, two-mass model with the identified parameters and with nominal parameters). The result clearly shows the benefits of parameter identification in constructing the two-mass model for a quarter-car system. The identified two-mass model is very close to the original model. On the other hand, the nominal model (dotted line) is far from the original system.

5 EFFECT OF SUSPENSION STRUCTURES ON THE EQUIVALENT PARAMETERS

In the previous sections, a set of equivalent parameters for a double wishbone type suspension system was obtained. Now, the same procedure is followed for the MacPherson-type suspension system. This is done in

Table 5 The equivalent parameters from a reduced-order model and an ARX model with component data

	$\hat{k}_s$ (N/m)	$\hat{b}_s$ (Ns/m)	$\hat{m}_s$ (kg)	$\hat{m}_u$ (kg)	$\hat{k}_t$ (N/m)
Model 1	36 537	2167.8	660.48	132.82	331 790
ARX model	36 546	2167.8	660.76	133.52	332 530
Component data	37 278	3000	404	45.24	186 390

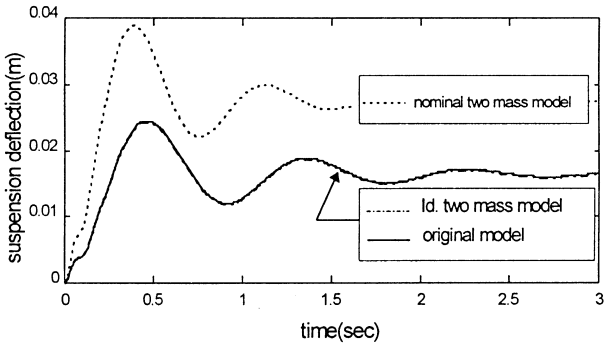

Fig. 13 The comparison of the responses (the identified two-mass model, nominal two-mass model and the original system)

order to demonstrate the effect of the suspension kinematic structure on the equivalent parameters.

The MacPherson-type suspension system is one of the most popular systems adopted for passenger car front suspension. An ADAMS model for the system is shown in Fig. 14.

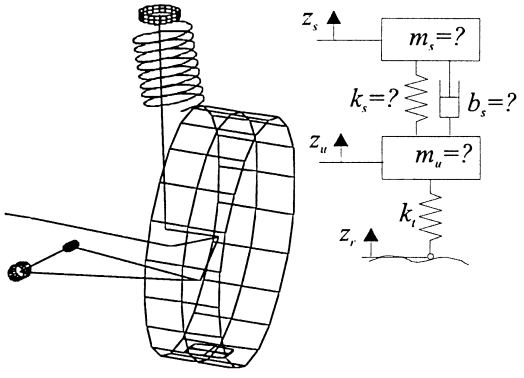

Fig. 14 MacPherson-type suspension system

The identified values of the suspension parameters for the system are shown in Table 6. In order to see the effect of the joint properties (e.g. kinematic joints or bushing), both the kinematic model and the compliance model are used. In the kinematic model, all connecting elements are modelled as kinematic joints (e.g. revolutional joint, universal joint, spherical joint, etc.). In the compliance model, the lower arm and the strut are attached to the car body with bushing elements.

Notice that there is little difference between each set of parameters for the MacPherson-type suspension (Table 6) compared with the result for the double wishbone type suspension system (Table 4). This result can be inferred from the fact that the structure of MacPherson-type suspension is very similar to the structure of the two-mass model; i.e. the relative motions of the sprung mass and the unsprung mass are almost coaxial in the MacPherson-type suspension [**5**].

6 CONCLUSIONS

In this paper, an accurate reduced-order model for a quarter-car suspension system is obtained. Linearization and model reduction techniques are used to find the reduced system from a complex quarter-car model. Using the approach described in the paper, a suspension model even with complex linkage layouts can be reduced to a simple model with reasonable accuracy.

On the basis of the results of model reduction, a set of equivalent parameters of the typical two-mass model is identified. The results reveal that the two-mass model is effective in representing a quarter-car system as long as an accurate set of identified parameters is determined. To this end, a convenient procedure to calculate the equivalent parameters from the characteristic equation of the reduced system is proposed.

Table 6 Identified equivalent parameters for a MacPherson-type suspension system

	$\hat{k}_s$ (N/m)	$\hat{b}_s$ (N s/m)	$\hat{m}_s$ (kg)	$\hat{m}_u$ (kg)	$\hat{k}_t$ (N/m)
Kinematic model	22 856	2758.9	434.51	34.461	195 920
Compliance model	25 017	2745.1	435.0	32.432	195 870
Component data	21 562	2940	404	42.0	186 220

An experimental way to obtain the equivalent parameters is suggested. It is based on system identification using two measured signals of the actuator input and suspension deflection.

Finally, the effect of the suspension structure on the equivalent parameters is investigated. The result shows that the identification process is essential for a complex suspension system such as the double wishbone type, whereas the benefits are not fully realized for less complex systems such as the MacPherson type.

An accurate reduced-order model may provide a more efficient way of designing a control system than a nominal model; i.e. the tuning process after applying the control system to the real system can be reduced. This may reduce the time and cost in the process of designing a control system.

The same technique may be extended to a full-car model for ride and handling analysis. If tyre lateral and longitudinal properties are included, a more accurate set of equivalent parameters may be obtained. Also, treating non-linear characteristics of the reduced-order system (e.g. asymmetric damping rate, non-linear spring stiffness, etc.) would be an interesting topic for obtaining more accurate simple models.

REFERENCES

1 **Thompson, A. G.** Design of active suspension. *Proc. Instn Mech. Engrs*, 1970–1, **185** (36), 553–563.
2 **Karnopp, D. C.** Active damping in road vehicle suspension systems. *Veh. System Dynamics*, 1982, **11**.
3 **Alleyne, A.** and **Hedrick J. K.** Nonlinear adaptive control of active suspensions. *IEEE Trans. Control Systems Technol.* 1995, **3**(1), 94–101.
4 **Kim, C.** and **Ro, P. I.** A sliding mode controller for vehicle active suspension systems with non-linearities. *Proc. Instn Mech. Engrs, Part D, Journal of Automobile Engineering*, 1998, **212**(D2), 79–92.
5 **Kim, C., Ro, P. I.** and **Kim, H.** Effect of suspension structure on equivalent suspension parameters. *Proc. Instn Mech. Engrs, Part D, Journal of Automobile Engineering*, 1999, **213**(D5), 457–470.
6 **Davison, E. J.** A method for simplifying linear dynamic systems. *IEEE Trans. Autom. Control*, 1966, **11**, 93–101.
7 **Chen, C. F.** and **Shieh, L. S.** A novel approach to linear model simplifications. *Int. J. Control*, 1968, **8**(6), 561–570.
8 **Bonvin, D.** and **Mellichamp, D. A.** A unified derivation and critical review of modal approaches to model reduction. *Int. J. Control*, 1982, **35**, 829–848.
9 **Kokotovic, R. E., O'Malley, R. E.** and **Sannuti, P.** Singular perturbations and order reduction in control theory—an overview. *Automatica*, 1976, **1**, 123–132.
10 **Moore, B.C.** Principal component analysis in linear systems: controllability, observability, and model reduction. *IEEE Trans. Automat. Control*, 1981, **26**, 17–32.

APPENDIX

An algorithm to calculate equivalent parameters for the two-mass system

The transfer function from the actuator control force, u, to the suspension deflection, $z_s - z_u$, for the two-mass system is as follows:

$$\frac{z_s - z_u}{u} = \frac{(m_s + m_u)s^2/(m_s m_u) + k_t/(m_s m_u)}{\Delta} \tag{19}$$

where

$$\Delta = s^4 + \left(\frac{m_s + m_u}{m_s m_u}\, b_s\right)s^3 + \frac{m_s(k_s + k_t) + m_u k_s}{m_s m_u}\, s^2 + \frac{b_s b_t}{m_s m_u}\, s + \frac{k_s k_t}{m_s m_u} \tag{20}$$

The same transfer function calculated from the reduced-order model is as follows:

$$\frac{z_s - z_u}{u} = \frac{b_2 s^2 + b_1 s + b_0}{s^4 + a_3 s^3 + a_2 s^2 + a_1 s + a_0} \tag{21}$$

1. Matching the steady states of $z_{sus}(t = \infty)$, $b_0/a_0 = 1/k_s$,

$$\hat{k}_s = \frac{a_0}{b_0} \tag{22}$$

2. From $a_0 = \hat{k}_s k_t/(m_s m_u)$,

$$\frac{k_t}{m_s m_u} = \frac{a_0}{\hat{k}_s} = \frac{a_0}{a_0/b_0} = b_0 \tag{23}$$

3. From $a_1 = \hat{b}_s k_t/(m_s m_u)$,

$$a_1 = \frac{\hat{b}_s k_t}{m_s m_u} = \hat{b}_s b_0 \tag{24}$$

or

$$\hat{b}_s = \frac{a_1}{b_0} \tag{25}$$

4. From $a_3 = [(m_s + m_u)/(m_s m_u)]b_s$,

$$\frac{m_s + m_u}{m_s m_u} = \frac{a_3}{\hat{b}_s} \tag{26}$$

5. From $[(m_s + m_u)/(m_s m_u)]k_s + m_s k_t/(m_s m_u) = a_2$,

$$m_s\left(\frac{k_t}{m_s m_u}\right) = a_2 - \left(\frac{a_3}{\hat{b}_s}\right)\hat{k}_s \tag{27}$$

or

$$m_s\left(\frac{k_t}{m_s m_u}\right) = \frac{a_2 - (a_3/\hat{b}_s)\hat{k}_s}{b_0} \tag{28}$$

6. From $(m_s + m_u)/(m_s m_u) = 1/m_u + 1/m_s = a_3/\hat{b}_s$,

$$\hat{m}_u = \frac{1}{a_3/\hat{b}_s - 1/\hat{m}_s} \tag{29}$$

7. From the result of step 2,

$$\hat{k}_t = b_0 \hat{m}_s \hat{m}_u \tag{30}$$